

Measurements of mechanical properties of discontinuities by rheological tests

FENG LI^{a,b}, XUAN WANG^{c,*}, BINBIN SHI^d, YONGFEI XUE^a, KECHAO ZHAO^a

^a School of Civil Engineering, Henan Institute of Engineering, Zhengzhou, Henan 451191, China

^b Henan Huaan Construction Co., Ltd. Taihang Road No. 48, Linzhou City, Henan 456550, China

^c School of Civil Engineering, Henan Polytechnic University, Jiaozuo, Henan 454000, China

^d School of Arts and Design, Henan Institute of Engineering, Zhengzhou, Henan 451191, China

The stress state, deformation and failure characteristics of rock discontinuity are constantly changing over time under long-term loads, exhibiting significant time effect. The time-dependent deformation and long-term strength of the rock mass are controlled significantly by the creep mechanical behavior of the discontinuities, and the study of creep properties of the rock mass discontinuities is an important area. According to Barton's standard profiles, this study adopted the first (JRC=0-2), fourth (JRC = 6-8), and tenth (JRC = 18-20) profiles to prepare the specimens of discontinuity. A series of shear tests and shear creep tests were carried out on the specimens. According to the test results, the failure state and mechanisms of rock discontinuity under shearing condition were analyzed. Furthermore, the method for identifying the long-term strength of discontinuity with different surface roughness was investigated. The long-term strength of rock discontinuity was compared to its instantaneous strength, and some valuable conclusions were obtained.

(Received January 06, 2015; accepted April 05, 2016)

Keywords: Discontinuity, Creep, Long-term strength

1. Introduction

Rock mass often contains discontinuity with different characteristics and degrees of development due to the combinatorial effects of inherent stress, groundwater, weathering, and many other factors, and therefore exhibits discontinuity, heterogeneity and anisotropy. Generally, the stability of engineering rock largely depends on the degree of development of the discontinuity and its mechanical properties. As a complex geological mass, one of the most important mechanical properties for rock discontinuity is the creep property [1]. Engineering rock creep failure is very common, e.g., creep rupture occurred several decades after the highway tunnel excavation; long-term creep deformation of the weak discontinuity, silted intercalation, or fault fracture zone led to sliding failure of rock slope, etc.

The stress state, deformation and failure characteristics of rock discontinuity are constantly changing over time under long-term load, exhibiting significant time effect [2]. Therefore, it is necessary to perform in-depth analysis and study on the creep property and the method to determine the long-term strength of rock mass. Bieniawski (1967) [3, 4] proposed that the long-term uniaxial compressive strength of rock was

determined by the turning point on the stress-volume strain curve that marks the transition from stable to unstable crack propagation. Munday (1977) [5] investigated sandstone, marble rock, granodiorite and granite through volume expansion method and maximum Poisson's ratio method, and found that the long-term strength obtained through the latter method was higher than that obtained from the former. Bowden (1984) [6] from the University of Toronto and found that the creep property of rock discontinuity was similar to that of intact rock. Lajtai (1991) [7] studied the relationship between the loading rate and strength of rock using time-dependent strength method, and found that the effects of both loading rate and the experimental condition on the strength of rock specimens are systematic and predictable. According to the rheological test of weak intercalated layers and corresponding theory, Liu (1996) [8] proposed an approach to determine the long-term strength through rheological test. Liu (2000) [9] carried out rheological test on the plaster rock specimens from a gypsum mine using rock torsional rheometer, and concluded that the long-term strength of anhydrite was 66% of its instantaneous strength. Cui (2006) [10] developed the gravitation level style rock rheometer, and performed uniaxial compression

experiment on red sandstone specimens using it to investigate the creep property.

The creep properties of rock discontinuity are affected by its complex surface configuration, undulate form, level of roughness, and many other factors [11]. According to Barton's standard profiles, this study adopts the first (JRC = 0-2), fourth (JRC = 6-8), and tenth (JRC = 18-20) profiles to prepare the discontinuity specimens. Shear test and shear creep test were conducted. Based on the results, the failure state and mechanisms of rock discontinuity under shear creep test were analyzed. Meanwhile, the method for deterring the long-term strength of discontinuity with different JRCs was studied and compared to the conventional strength.

2. Testing facility and specimen preparation

The CSS-1950 biaxial rheological testing machine was implemented for the creep test (Fig.1). This machine can be applied separately or simultaneously on vertical axis compression load and also horizontal axis compression load. The loading system used a servo-controlled motor and ball screw system. The maximum compression load for the vertical axis was 500KN, and the load for the horizontal axis was 300KN. The load control stability was smaller than 1% indication. This can fully satisfy the test accuracy requirements for this study. The creep tests were equipped with four linear variable differential transformers (LVDT) for the strain measurement with accuracy of 0.5%. The stress was measured using a 1.0MN capacity load cell. The creep tests were carried out in the lab with constant temperature and humidity. The temperature was controlled at $(20\pm 1)^{\circ}\text{C}$ to reduce the impact of thermal factors on the test results. The specimen was placed between the top and bottom platens after fixing the LVDTs to it. The external loading was applied stepwise until failure. If the specimen did not fail at the predicted stress level, the load continued being applied until it failed.



Fig. 1 CSS-1950 rock rheology biaxial testing machine (image by Zhang et al.)

According to Barton's standard profiles, this study adopted the first (JRC = 0-2), fourth (JRC = 6-8), and tenth (JRC = 18-20) profiles to prepare the discontinuity specimens. The specimens were made of cement, standard sand, and water. In order to ensure the quality and enhance the density of the specimens, stratified charge and layered tamping were adopted during the pouring process (Fig. 2). The compressive strength of cubic specimens, the normal shear strength and shear creep properties were tested. In the unconfined compression test, five cubic specimens were tested and the compressive strength was obtained by taking the average of the five.

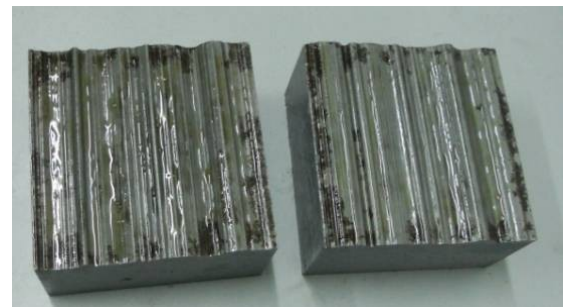


Fig. 2 The steel model of Barton's standard profiles and the specimen (image by Zhang et al.)

Shear creep tests were adopted for this study, and the shear creep tests were carried out in the National Key Lab in Tongji University. The multi-level loading on a single specimen was used for this creep test. Before the creep tests, the mechanical properties of rock samples were firstly tested. Then the creep tests could be performed based on the pre-confirmed stress levels. Based on the results from conventional shear tests, shear creep tests were carried out with specimens of different roughness. Three specimens with different roughness were subject to three different levels of normal stress (10%, 20% and 30% of the uniaxial compressive strength). A five-step loading process (50%, 60%, 70%, 80%, and 90% of the shear strength obtained from the conventional shear tests) was adopted, and each stress level lasted for three days.

3. Result analysis

3.1 Conventional shear test

Before conventional shear test, the uniaxial compression tests for cubic specimens without discontinuity were carried out to determine the uniaxial compression strength (UCS) of the specimens. The failure state of the cubic specimens in the unconfined compression test was mostly columnar or pyramid-shaped splitting failure. Some specimen clearly exhibited necking failure in the middle. According to the test data, the average value of compressive strength was 21.73MPa, which was then taken as the basis for determination of axial loading in the conventional shear test and shear creep test.



Fig. 3 Failure specimens during uniaxial compression tests.

The normal stresses in the conventional shear tests were 10%, 15%, 20%, 30%, and 40% of the UCS, which were 2.17MPa, 3.26MPa, 4.35MPa, 6.52MPa, and 8.69MPa, respectively. The typical shear curves of discontinuities with different roughness and the curve fitting are plotted in Fig. 4.

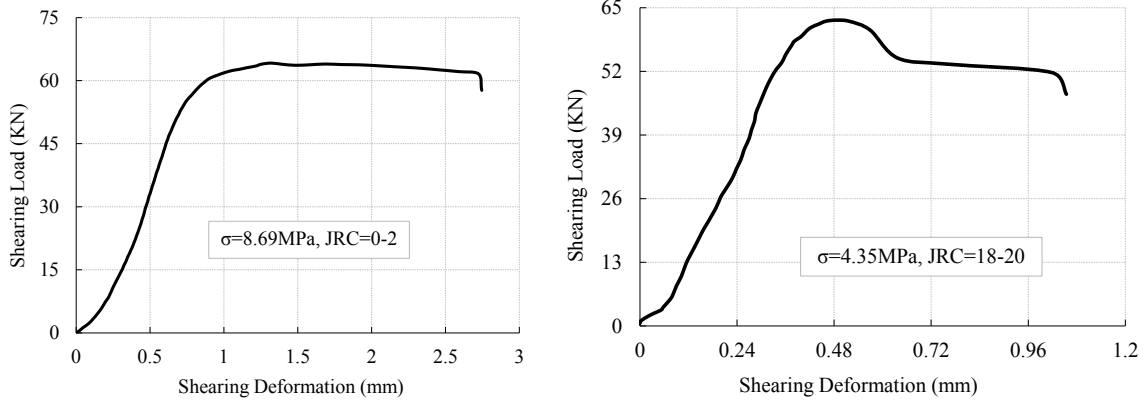


Fig. 4. The shearing curves and curve fitting of conventional shear test.

The failure state of discontinuity specimens with smaller roughness was mainly frictional sliding failure. The degree of friction was clearly related to the normal stress: the higher the normal stress, the higher the degree of friction. Discontinuity specimens with higher roughness always failed with surface projections sheared. Meanwhile, clear frictional marks could be observed on the discontinuity surface. The discontinuity shear strength parameters are shown in Table 1.

Table 1. The shear strength parameters of discontinuity specimens.

JRC	C _j (MPa)	φ _j (°)
0-2	0.55	34
6-8	0.61	37
18-20	1.13	47

3.2 Shear creep test

Based on the results from compressive strength tests and the conventional shear tests, shear creep tests were

carried out by adopting the first, fourth, and tenth Barton’s standard profiles for preparing the specimen of discontinuity. The normal stresses were 0.1UCS, 0.2UCS, and 0.3UCS (the corresponding values are 2.17MPa, 4.35MPa, and 6.52MPa, respectively). The horizontal shear stresses are 50%, 60%, 70%, 80%, and 90% of the shear strength obtained from the conventional shear test, and adjusted according to the deformation during the process of testing.

In the shear creep tests, a group of specimens with the same roughness was first selected, and normal stress was exerted. When the normal deformation became steady, a shear force was exerted and maintained at a constant level. The creep deformation of the discontinuity under each level of shear stress was measured until the deformation tended steady. Each level of loading lasted for three days until the specimen failed. While the last level of loading was exerted, once the shear creep displacement started to increase quickly with time, the frequency of observation should be increased in order to better record the last stage of the creep failure. The typical shear creep curves of the specimens with different roughness are shown in Fig.5.

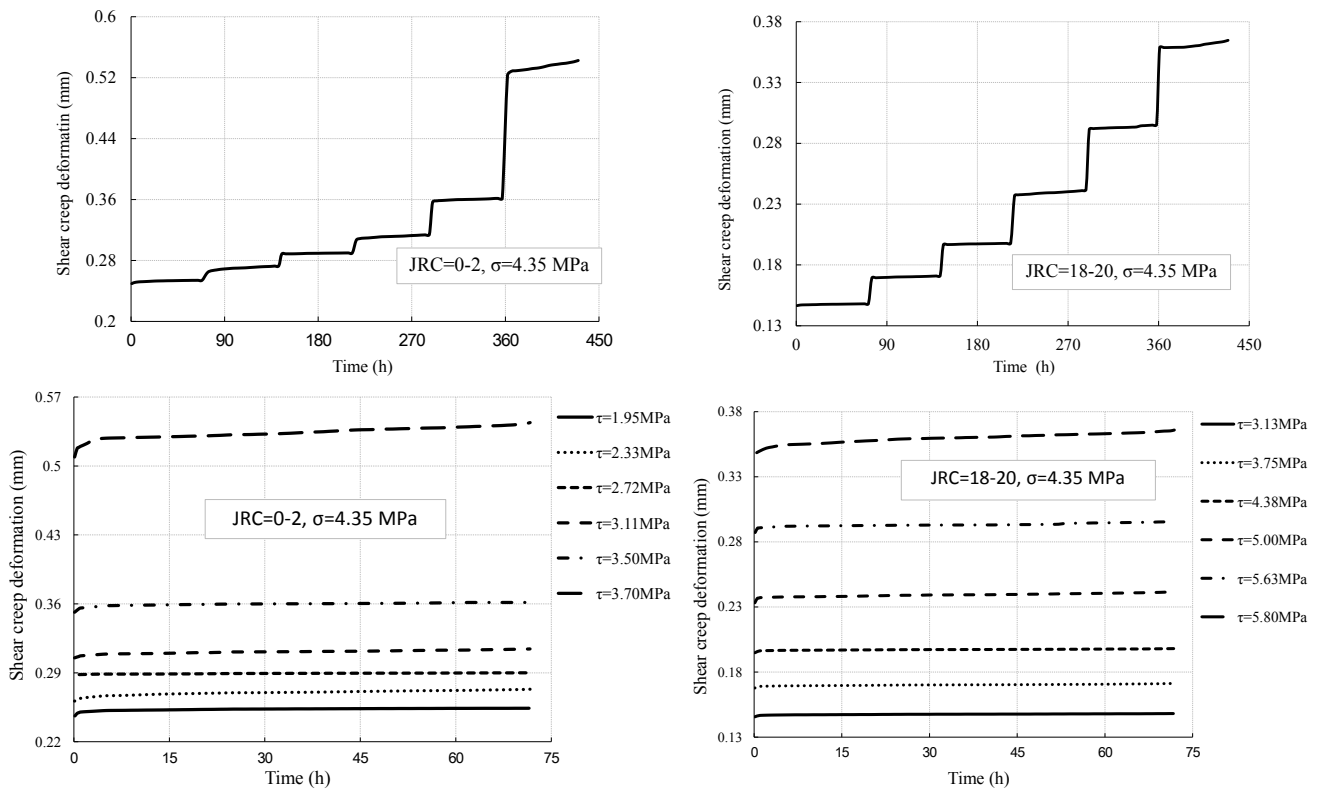


Fig. 5. Creep curves of the specimens under different normal stresses.

According to the shear creep curves, instantaneous deformation can be clearly observed. Accelerated creep did not occur under the last level of shear loading. When the shear stress reached a certain level, the discontinuity quickly slipped and failed. The duration of failure was very short [12,13]. The reason is that during the creeping, the upper and lower pieces of the discontinuity specimen developed relative displacement in the way of overriding or shearing. High viscous resistance was generated between the upper and lower pieces, and a certain level of stress is required to overcome this resistance. When shear stress is larger than this level of stress, the viscous resistance decreases promptly and the specimen will have large shear displacement within a very short period of time and then quickly fail. Compared to intact rock, shear creep of discontinuity showed obvious instantaneous deformation, which was closely related to the normal stress and shear stress. The higher the normal stress, the

larger the instantaneous displacement observed.

According to the failure state of discontinuity (Fig. 6), discontinuity with lower roughness mainly showed sliding failure after the viscous resistance disappears, since most of the surface projections were cut in the test. Discontinuity with higher roughness failed due to that the large surface projections were sheared. The projections of the upper and lower pieces of the discontinuity were engaged more closely under long-term constant normal load and incremental shear load. During the shear creep, there is always a relatively high shear stress exerted on the discontinuity surface projections. The projections are cut off under the last level of shear load, and the part that was cut off from one piece was embedded into the other piece, which is clearly shear failure. Overriding or sliding failure was not observed.

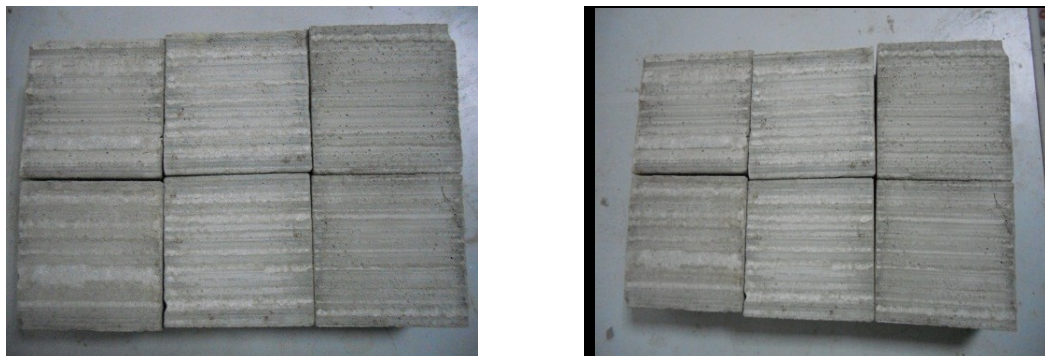


Fig. 6. Fracture characteristics of the test specimen (image by Zhang et al.).

3.3 Shear creep model

Theoretical creep model has many different forms. Before selecting a suitable one, it is necessary to analyse the creep curve of the specific material [14]. By observing the creep curve of discontinuity with different roughness, it is not difficult to find out that before reaching the yield stress the creep curve has three characteristics: (1) instantaneous elastic strain immediately occurs when instantaneous stress is exerted; (2) the strain tends to increase with time; (3) creep deformation will eventually become steady under each level of loading, and no accelerated creep are observed during the entire testing process.

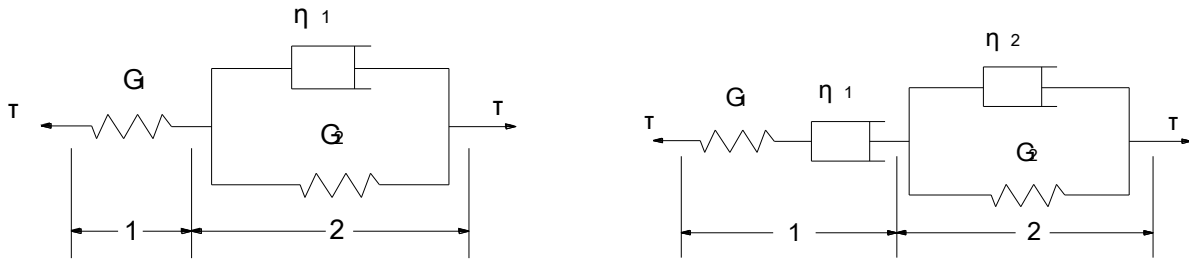


Fig. 7 The generalized Kelvin Model and the Burgers model

Under the shear creep condition, the equations of generalised Kelvin's model (Eq.1) and Burgers' model (Eq.2) are as follows.

$$u = \tau \left\{ \frac{1}{G_1} + \frac{1}{G_2} \left[1 - \exp\left(-\frac{G_2}{\eta_1} t\right) \right] \right\}. \quad (1)$$

$$u = \tau \left\{ \frac{1}{G_1} + \frac{t}{\eta_1} + \frac{1}{G_2} \left[1 - \exp\left(-\frac{G_2}{\eta_2} t\right) \right] \right\}. \quad (2)$$

Where G_1 is the instantaneous deformation of the discontinuity, $1/\eta_1$ is the steady creep rate, and G_2/η_2 is the duration of the initial creep. The r -squared value (i.e. R^2) is above 0.95 when generalised Kelvin's model and Burgers' model are adopted for curve-fitting, so the goodness of fit is relatively high.

According to the results of curve-fitting, attenuated creep can be observed under the first two levels of shear stress. Steady creep stage starts to exhibit from the third level of shear stress. The second and third levels of shear stress are 60% and 70% of the conventional ultimate shear strength of the corresponding discontinuity, respectively. Therefore, it is between 60%-70% of conventional shear

strength under which a specimen of discontinuity transits from attenuated creep stage to steady creep stage. According to these properties, it can be seen that the discontinuity has typical visco-elasticity, i.e., the creep strain increases with time. Instantaneous creep stage and steady creep stage are both clearly exhibited, but the steady creep stage dominates. Accelerated creep stage was not observed during the entire process and the failure is abrupt. Based on the creep property reflected by the curve, generalised Kelvin model and Burgers model (Fig. 7) provide good description of the creep properties of the discontinuity. The specimens of discontinuity show attenuated creep under the first two levels of shear stress, which can be described by the generalized Kelvin model. The specimens show steady creep from the third level of shear stress, which can be described by Burgers model.

strength under which a specimen of discontinuity transits from attenuated creep stage to steady creep stage.

4. The long-term strength of discontinuity

During the creeping of discontinuity under multi-step loading, we observed that there was always a critical stress [15-17]. If the shear stress was lower than the critical stress, the steady creep rate tended to be zero and the specimen could not fail. If the shear stress was higher than it, the specimen would eventually fail after creep deformation. We defined this critical stress as the long-term strength of discontinuity. Most discontinuity of engineering rock mass is subject to a shear stress field; therefore, it is crucial to understand how to determine its long-term strength and to predict the time during which it is safe to use.

4.1 Determination of long-term strength of discontinuity using creep rate

Rock discontinuity shows different deformation process and creep rate under different shear stress. The long-term strength of discontinuity can be obtained by: (1) identifying the stress state at which the attenuated creep stage transits to the steady creep stage (i.e., identifying the

critical point on the creep test curve at which one stage transits to the other); (2) curve-fitting to obtain the shear stress-time curve.

Taking the specimen prepared according to Barton's fourth standard profile (JRC=6-8) as an example, under normal stress $\sigma=2.17\text{MPa}$, the specimen exhibits attenuated creep when shear stresses $\tau=1.10\text{MPa}$ and $\tau=1.32\text{MPa}$; the specimen exhibits steady creep when $\tau=1.54\text{MPa}$, $\tau=1.76\text{MPa}$, and $\tau=1.98\text{MPa}$ (Fig. 8). The transition durations between attenuated creep and steady creep for $\tau=1.54\text{MPa}$, $\tau=1.76\text{MPa}$, and $\tau=1.98\text{MPa}$ are 6.7 h, 13.3 h, and 29.1 h, respectively. The equation $\tau = a + b e^{-ct}$ is deployed for fitting the shear stress-time curve. When time tends to infinity, the shear stress becomes a steady constant, which is the long-term strength. In this equation, a is the long-term strength when time tends to infinity. Therefore, the long-term strength of the discontinuity specimen prepared according to Barton's fourth standard profile under $\sigma=2.17\text{MPa}$ is 1.48MPa.

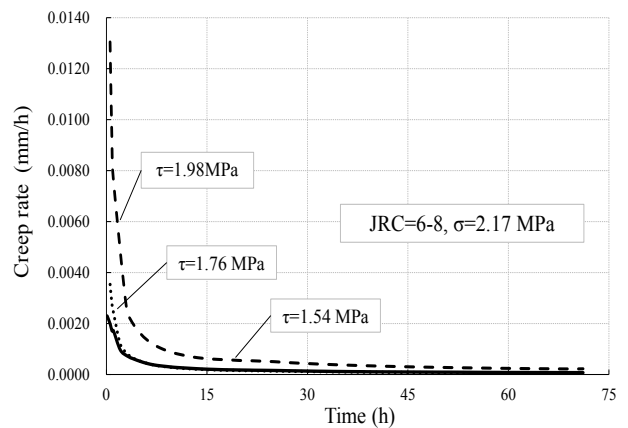


Fig. 8. Creep rate deviation curves of the test specimens.

In the method described above, the long-term strength of the specimen of discontinuity prepared according to Barton's first (JRC = 0-2), fourth (JRC = 6-8), and tenth (JRC = 18-20) standard profiles can be obtained (Table 2).

Table 2. The long-term strength using creep rate.

Discontinuities	σ (MPa)	Long-term strength (MPa)	The ratio between Long-term strength and normal strength
JRC=0-2	2.17	2.17	67.88%
	4.35	4.35	68.97%
	6.52	6.52	68.39%
JRC=6-8	2.17	2.17	67.33%
	4.35	4.35	66.88%
	6.52	6.52	67.75%
JRC=18-20	2.17	2.17	68.27%
	4.35	4.35	68.40%
	6.52	6.52	67.76%

4.2 Determination of long-term strength of discontinuity using the transition creep law

According to the transition creep law, during the rock discontinuity creeping process the rock mass will not fail and only exhibit attenuated creep if the external load is below a certain level; once the external load is above that certain level, steady creep can be observed and the rock mass will eventually fail under the long-term load at this level. Generally, it is very difficult to record the exact value of this load at which transitional creep occurs, but an interval can be obtained and hence used as the long-term strength of the rock discontinuity.

In this shear creep test of discontinuity, it is found that generalised Kelvin's model is more suitable for shear creep curve fitting in the stage when only attenuated creep

occurs, while Burger's model is more suitable for the steady creep stage. Specimens of discontinuity only exhibited attenuated creep under the first two levels of shear stress, and steady creep started to show from the third level of shear stress. Therefore, the long-term strength interval could be taken as the range between the level of shear stress at which steady creep first exhibits and the last level. Taking the specimen prepared according to Barton's fourth standard profile (JRC=6-8) as an example, when the normal stress $\sigma=2.17\text{MPa}$, attenuated creep only exhibited at $\tau=1.10\text{MPa}$ and $\tau=1.32\text{MPa}$. Steady creep exhibited at $\tau=1.54\text{MPa}$, $\tau=1.76\text{MPa}$, and $\tau=1.98\text{MPa}$. Therefore, the interval [1.32MPa, 1.54MPa] can be considered as the long-term strength interval of the specimen $\sigma=2.17\text{MPa}$. Similarly, the long-term strength of other specimens are obtained and shown in Table 3.

Table 3. The long-term strength using transition creep law.

Discontinuities	σ (MPa)	Long-term strength (MPa)	The ratio between Long-term strength and normal strength
JRC=0-2	2.17	[1.06 , 1.23]	60%-70%
	4.35	[2.33 , 2.72]	60%-70%
	6.52	[2.84 , 3.31]	60%-70%
JRC=6-8	2.17	[1.32 , 1.54]	60%-70%
	4.35	[2.72 , 3.18]	60%-70%
	6.52	[3.19 , 3.72]	60%-70%
JRC=18-20	2.17	[2.15 , 2.51]	60%-70%
	4.35	[3.75 , 4.38]	60%-70%
	6.52	[4.74 , 5.53]	60%-70%

According to the results from this shear creep test, the ratio between the long-term strength and the conventional shear strength is between 60% and 70%. The long-term strength obtained through the creep rate law is within the long-term strength interval obtained from the transition creep law, so the difference is minimal.

5. Conclusions

This study performed shear test and shear creep test on specimens with different surface roughness. A wealth of experimental data was obtained, based on which the creep property and long-term strength of rock discontinuity are investigated. The main conclusions can be drawn as follows:

(1) In the shear creep test, the shear creep curve only includes attenuated and steady creep stages, while accelerated creep is not observed. Generalized Kelvin's model should be used for curve fitting for the attenuated creep stage, and the Burgers' model can be used for the steady creep stage.

(2) During the shear creeping of specimens with different roughness, a relatively high shear stress is always exerted on the surface projections. The projections are eventually cut off, which is clearly shear failure rather than overriding or sliding failure.

(3) The long-term strength is determined through the creep rate law and the transition creep law. The long-term strength is 60%-70% of the conventional shear strength. The long-term strength obtained through the transition creep law is an interval, and the long-term strength obtained through the creep rate law is within this interval.

Acknowledgments

Thanks for the financial support given by the National Comprehensive Reform Pilot Project of Civil Engineering. The research is also supported by the Natural Science Research Project of Education Department of Henan Province (No. 2010A560006, 2011B510002).

References

- [1] Q.Z. Zhang, M.R. Shen, W.Q. Ding, C. Carl J Geophy Eng, **9**(2), 210 (2012).
- [2] D.F. Malan, Rock Mech Rock Eng, **32**(2), 123 (1999).
- [3] Z.T. Bieniawski, Int J Rock Mech Min Sci, **4**(4), 395 (1967).
- [4] Z.T. Bieniawski, Eng Geo, **2**(3), 149 (1967).
- [5] J.G.L. Munday, A.E. Mohamed, R.K. Dhir, Conference 'Rock Engineering' University of Newcastle-upon-Tyne, p. 127 (1977).
- [6] R.K. Bowden, Time-dependent behaviour of joints in shale, M.A.Sc. Thesis, University of Toronto, Ontario, (1984).
- [7] E.Z. Lajtai, Geotech and Geolo Eng, **9**(2), 109 (1991).
- [8] J.H. Liu, C.S. Wang, H.H. Yang, Site Inv Sci Tech, **5**, 3 (1996).
- [9] M.Y. Liu, C.Y. Xu, Chi Min Mag, **9**(2), 53 (2000).
- [10] X.H. Cui, Z.L. Fu, Chin J Rock Mech Eng, **25**(5), 1021 (2006).
- [11] S.Q. Yang, Experimental study on rheology damage and failure mechanical behavior of rock under complex States. Nanjing: Hohai University, 2008.
- [12] C.H. Yang, J.J.K. Daemen, J.H. Yin, Int J Rock Mech Min Sci, **36**(2), 233 (1999).
- [13] Q.Z. Zhang, M.R. Shen, Z. Wen, J Mate in Civil Eng, **23**(8), 1220 (2011).
- [14] D.F. Malan, Rock Mech Rock Eng, **35**(4), 225 (2002).
- [15] W.Y. Xu, S.Q. Yang, W.J. Chu, Chin J Rock Mech Eng, **25**(3), 433 (2006)
- [16] W.Z. Chen, X.J. Tan, S.P. Lu, J.P. Yang, G.J. Wu, H.D. Yu, et al, Chin J Rock Mech Eng, **28**(9), 1735 (2009)..
- [17] L. Ma, J.J.K. Daemen, Int J Rock Mech Min Sci, **43**, 282 (2006).

*Corresponding author: zhang_baogu@126.com